Equation of state of warm dense deuterium and its isotopes from density-functional theory molecular dynamics

J.-F. Danel, L. Kazandjian, and R. Piron

CEA, DAM, DIF, F-91297 Arpajon, France

Of the two approaches of density-functional theory molecular dynamics, quantum molecular dynamics is limited at high temperature by computational cost whereas orbital-free molecular dynamics, based on an approximation of the kinetic electronic free energy, can be implemented in this domain. In the case of deuterium, it is shown how orbital-free molecular dynamics can be regarded as the limit of quantum molecular dynamics at high temperature for the calculation of the equation of state. To this end, accurate quantum molecular dynamics calculations are performed up to 20 eV at mass densities as low as 0.5 g/cm^3 and up to 10 eV at mass densities as low as 0.2 g/cm^3. As a result, the limitation in temperature so far attributed to quantum molecular dynamics is overcome and an approach combining quantum and orbital-free molecular dynamics is used to construct an equation of state of deuterium. The thermodynamic domain addressed is that of the fluid phase above 1 eV and 0.2 g/cm^3. Both pressure and internal energy are calculated as functions of temperature and mass density, and various exchange-correlation contributions are compared. The generalized gradient approximation of the exchange-correlation functional, corrected to approximately include the influence of temperature, is retained and the results obtained are compared to other approaches and to experimental shock data; in parts of the thermodynamic domain addressed, these results significantly differ from those obtained in other first-principles investigations which themselves disagree. The equations of state of hydrogen and tritium above 1 eV and above, respectively, 0.1 g/cm^3 and 0.3 g/cm^3, can be simply obtained by mass density scaling from the results found for deuterium. This *ab initio* approach allows one to consistently cover a very large domain of temperature on the domain of mass density outlined above.

I. INTRODUCTION

Hydrogen, the most abundant element in the universe, has an obvious interest for models of stellar and planetary interiors. Its isotopes, deuterium and tritium, play a central role in inertial confinement fusion where they are used as targets; in this case, the thermodynamic domain of interest covers densities ranging from 0.1 to 1000 g/cm^3 and from a few electronvolts to several hundred electronvolts, as noted by Hu *et al.* [1]. In the context of these applications, the equation of state (EOS) that determines pressure and internal energy as a function of mass density and temperature is an important part of the modeling. Until recently, the EOSs of hydrogen and of its isotopes have been based on chemical models [2–5] that describe the system in terms of well-defined chemical species interacting through pairwise potentials; the difficulty with such models is that, in the thermodynamic domain of interest, there is no clear definition of the chemical species present. Then, in order to use a reliable approach, it is necessary to implement *ab initio* calculations in which a system is regarded as a mixture of electrons and nuclei interacting through Coulombic interactions.

Among the *ab initio* approaches already applied to hydrogen, coupled electron-ion Monte Carlo (CEIMC), which assumes electrons to be in their ground state, has been used below 1 eV at densities of the order of 1 g/cm^3 [6]. In another *ab initio* approach applied to hydrogen and deuterium, path integral Monte Carlo (PIMC), electrons and ions are treated on the same footing and the quantum effects of both species are taken into account [1,7–9]. PIMC loses its efficiency at low temperature, typically below one-tenth of the Fermi temperature [1]. A third *ab initio* approach,

quantum molecular dynamics (QMD), has also been applied to hydrogen and deuterium [10–15]. This approach combines classical molecular dynamics for nuclei [16] and density-functional theory for electrons [17–20]. It is the version of density-functional theory molecular dynamics (DFT-MD) that implements a quantum treatment of electrons; as a result, apart from general hypotheses, the only approximation involved in QMD lies in the choice of the exchange-correlation functional.

Because of the Fermi-Dirac distribution of the electronic quantum states involved in QMD, its application has been restricted to low temperatures. As PIMC simulations become increasingly accurate as temperature increases, Caillabet *et al.* [15] have supplemented QMD results, obtained by themselves below 0.9 eV, with PIMC results in order to construct an EOS of the fluid phase of hydrogen up to 10 eV in the density range 0.2–5 g/cm^3. In the same spirit, QMD and PIMC are combined in Refs. [21] and [22] to provide a first-principles investigation of warm dense plasmas of carbon and neon.

It is possible to avoid the QMD limitation in the high-temperature regime by approximating the kinetic electronic free energy per unit volume by a function of the local electronic density and possibly of its gradient [20,23]. As electronic orbitals are no longer involved, the approach is called orbital-free molecular dynamics; it is another version of DFT-MD that is less computationally expensive than QMD. The approach without gradient correction is hereafter denoted OFMD, and the approach with the gradient correction is hereafter denoted OFWMD (with W standing for Weizsäcker). For the EOS of a boron plasma at densities of the order of the normal density, we have recently shown [24] that, as temperature increases at given density, OFWMD is the

limit of QMD apart from shell effects that can be taken into account with a fcc lattice of nuclei or with an average-atom model [25–28]. As a result, we have obtained a method reproducing QMD results up to high temperatures where QMD cannot be directly implemented [24]. The approach has been successfully extended to an element with a high atomic number such as lutetium [29].

The approach of Refs. [24] and [29] allows one to produce results at temperatures that are not accessible with CEIMC, because these temperatures are too high, or with PIMC, because they are too low. The purpose of the present paper is to include this approach in the construction of an EOS of warm dense deuterium and its isotopes in a large thermodynamic domain. This domain is that of the fluid phase above 1 eV and above 0.1 g/cm^3 for hydrogen, 0.2 g/cm^3 for deuterium, and 0.3 g/cm^3 for tritium. It can be noted that the DFT-MD results for EOSs of isotopes are connected through a mass density scaling described by Caillabet *et al.* [15]; as a result, it is sufficient for our purpose to construct a table for only one of the isotopes of H. We choose to focus on deuterium because of the abundance of PIMC data [1,7] that can be used for comparison.

The paper is organized as follows. Section II describes the QMD and orbital-free molecular dynamics formalisms. In Sec. III, the approach of Refs. [24] and [29] is applied to warm dense deuterium, discussed, and its sensitivity to exchange correlation is tested. The results obtained are compared to other EOSs of the literature and to shock experiments in Sec. IV. Section V presents our conclusions. Atomic units are used unless otherwise stated. The quantum average-atom calculations are performed with the VAAQP code that implements several average-atom modeling options [27]. All molecular dynamics simulations are performed with the electronic structure package ABINIT [30–32]. The calculations presented include QMD simulations at low mass density and high temperature that have been made possible by the parallelization efforts devoted to ABINIT [33].

II. FORMALISM AND COMPUTATIONAL DETAILS

The system is constructed by replication of a finite sample of N atoms in a basic cubic reference cell [16]. The nuclei are assumed to obey Boltzmann statistics [34]. In a given arrangement, they are subject to forces computed from the electronic density $n(\mathbf{r})$ by the Hellmann-Feynman theorem [20]. The electronic density is assumed to instantaneously adjust to the displacement of nuclei (Born-Oppenheimer approximation) and, according to density-functional theory [20], $n(\mathbf{r})$ at thermodynamic equilibrium is obtained by minimizing the electronic free energy F_e under the constraint of charge neutrality. At given volume V and temperature T, F_e is a functional of $n(\mathbf{r})$ equal to

$$F_e[n(\mathbf{r})] = F_0[n(\mathbf{r})] + F_{xc}[n(\mathbf{r})] + \frac{1}{2} \int_V \int_V \frac{n(\mathbf{r})n(\mathbf{r}')}{|\mathbf{r} - \mathbf{r}'|} \, d\mathbf{r} \, d\mathbf{r}' + \int_V n(\mathbf{r})v(\mathbf{r}) \, d\mathbf{r}, \qquad (1)$$

where $F_0[n(\mathbf{r})]$ is the free energy of a gas of noninteracting electrons with electronic density $n(\mathbf{r})$ in V at T, $F_{xc}[n(\mathbf{r})]$ is

the exchange-correlation contribution to the free energy in V at T, and $v(\mathbf{r})$ is the external potential acting on electrons (in the present case, it is due to nuclei).

At each time step, for a given arrangement of nuclei, $n(\mathbf{r})$ and the forces acting on them are computed and they are moved in the isokinetic ensemble [35,36] so that temperature can be regarded as exactly known. The statistical error is evaluated as indicated in Refs. [16] and [37].

A. Orbital-free molecular dynamics

In orbital-free molecular dynamics $F_0[n(\mathbf{r})]$ is assumed to be expressed by

$$F_0[n(\mathbf{r})] = \int_V \mathcal{F}_0(n) \, d\mathbf{r} + \int_V h(n) \, \frac{|\nabla n|^2}{n} \, d\mathbf{r}, \qquad (2)$$

where n in the integrals stands for $n(\mathbf{r})$ and $\mathcal{F}_0(n)$ is the free energy per unit volume of a homogeneous gas of noninteracting electrons of density n at temperature T [23]. $h(n)$ is a function of n implicitly depending on T in the OFWMD method [23] or is equal to 0 in the OFMD method.

The divergence of the electronic density in the vicinity of nuclei is suppressed by replacing the Coulombic electron-nucleus interaction by a regularized potential constructed, in the framework of the average-atom model, as explained in Refs. [38] and [39]. All parameters are determined by a systematic search of numerical convergence, within statistical error, of pressure and internal energy. The rules of thumb given in Ref. [40] have been used to choose the time step and the cutoff energy. All computations have been performed with $N = 32$ nuclei and $n_{\text{step}} = 2000$ time steps (after thermal equilibration) that we have found sufficient to ensure convergence for deuterium in the thermodynamic domain considered. In the calculation of the stress tensor [41], the kinetic term is simplified in the Thomas-Fermi framework, and the contribution of the gradient correction is treated as indicated by Dal Corso and Resta [42].

B. Quantum molecular dynamics

In QMD, the only difference with orbital-free molecular dynamics lies in the fully quantum approach of $F_0[n(\mathbf{r})]$; this approach allows an exact treatment of the inhomogeneity of $n(\mathbf{r})$. The free energy $F_0[n(\mathbf{r})]$ of a gas of noninteracting electrons is obtained by using finite-temperature density-functional theory [17–19]; at each time step, for a given arrangement of nuclei, the electronic density is searched as a decomposition in terms of one-electron orbitals [17–20]

$$n(\mathbf{r}) = \sum_{i,\mathbf{k}} f_{i,\mathbf{k}} |\Psi_{i,\mathbf{k}}(\mathbf{r})|^2, \qquad (3)$$

where i is an integer index designating a band, $\mathbf{k}$ designates a k point [43], $f_{i,\mathbf{k}}$ is an occupation number determined by a Fermi-Dirac distribution, and the $\Psi_{i,\mathbf{k}}$ are one-electron orbitals.

The electron-ion interaction is represented by a pseudopotential in the PAW formalism [44,45]. A pseudopotential is characterized by numerical parameters that must be included in the tests of numerical convergence. The augmentation radius r_{PAW} in particular must be chosen sufficiently small that the

spheres of radius r_{PAW} centered on nuclei do not overlap significantly during a simulation. Pseudopotentials are generated with the code ATOMPAW [46]. A norm-conserving Troullier-Martins scheme is used to construct a local pseudopotential from the all-electron effective potential and Blöchl's scheme is used to generate pseudo partial waves and associated projectors [46]. For a given arrangement of nuclei, the stress tensor is obtained as the derivative of the total free energy with respect to strain, as explained in Ref. [45].

All numerical parameters are determined by a systematic search of numerical convergence, within statistical error, of pressure and internal energy. In view of the relative smallness of the statistical error, this criterion of numerical convergence is demanding on the parameters to be used. For deuterium in the thermodynamic domain considered, the time step found for orbital-free molecular dynamics, as well as $N = 32$, $n_{\text{step}} = 2000$, and $r_{PAW} = 0.35$ a.u. (atomic units), has been found sufficient to ensure convergence.

III. CALCULATION OF THE EOS OF DEUTERIUM UP TO HIGH TEMPERATURE

We first compare the electronic pressures, defined as those calculated for a fcc lattice of nuclei in the quantum approach and as those calculated in the average-atom (AA) model [23] in the orbital-free approach. Then we show how the QMD EOS tends to the orbital-free EOS at high temperature along isochores, and we test the sensitivity of the EOS constructed to exchange correlation. For the calculations presented in Secs. III A and III B, the exchange-correlation contribution, denoted LDA (standing for local-density approximation), is taken equal to the sum of the exchange energy per unit volume of a gas of electrons at $T = 0$ K [20] and of the correlation energy per unit volume of an unpolarized gas of electrons proposed by Perdew and Wang [47].

A. Comparison of quantum and orbital-free electronic pressures

We define the electronic pressure in the orbital-free approach as the average-atom pressure [23]. In the thermodynamic domain considered, for the orbital-free approach, the relative difference between the AA and fcc pressures of deuterium is about 1% at the lowest temperature and mass density, and decreases as temperature and mass density increase, to less than 0.2% above 5 eV; incidentally, it can be noted that the Thomas-Fermi ion-in-cell model was proposed as an approximate treatment of electrons in a periodic lattice [48] before being applied to the nonperiodic plasma case [49]. In view of our definition of the electronic pressure in the orbital-free approach, the above result leads us to define the electronic pressure in the quantum approach as the fcc pressure. Then comparing the electronic pressures amounts to comparing the quantum and orbital-free pressures obtained with a given arrangement of nuclei, namely, a fcc lattice; the present section aims at this comparison. Apart from involving a single time step, the fcc lattice has the advantage of having symmetry properties and of being characterized by only $N = 4$ atoms; the resulting gain in computation time allows one to carry out the quantum
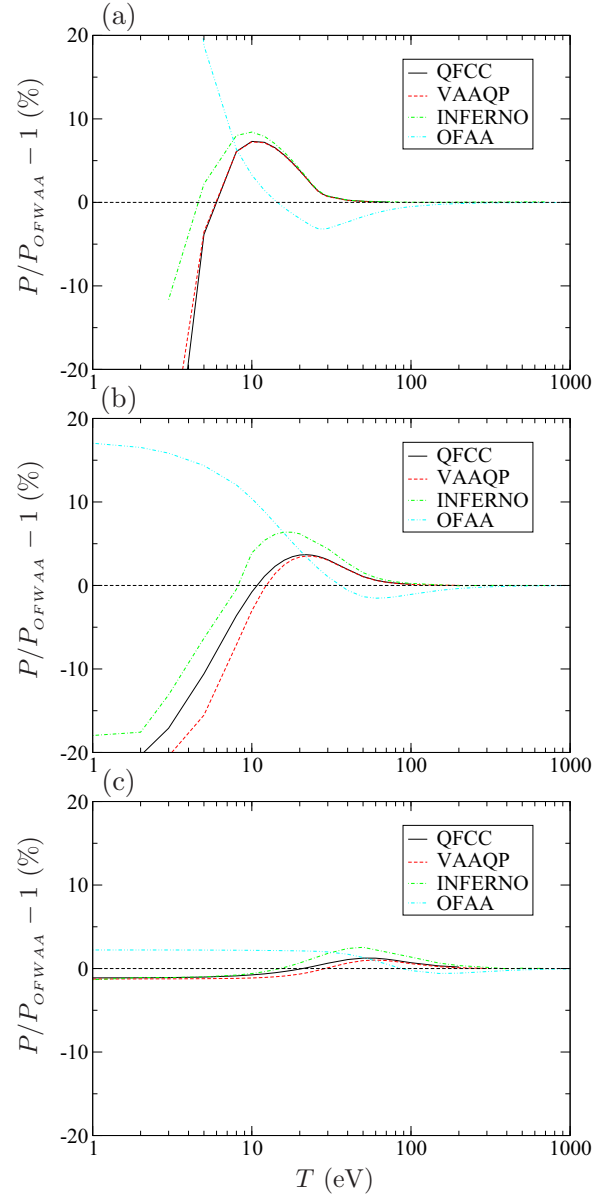
FIG. 1. Relative differences between the pressures P_{QFCC}, P_{VAAQP}, P_{INFERNO}, P_{OFAA}, and P_{OFWAA}, with the latter taken as the reference, at (a) 0.2 g/cm^3, (b) 2.5 g/cm^3, and (c) 20 g/cm^3 for deuterium. The results have been obtained with the LDA exchange-correlation functional.

approach and the comparison of electronic pressures at higher temperature.

In the following, electronic pressures are denoted OFAA for the orbital-free approach without gradient correction, OFWAA for the orbital-free approach with the gradient correction, and QFCC for the fcc pressure obtained with the quantum approach. The electronic pressures P_{OFAA}, P_{OFWAA}, and P_{QFCC} of deuterium are compared along the isochores 0.2, 2.5, and 20 g/cm^3 in Fig. 1. The domain of temperature where P_{QFCC} can be calculated increases when mass density increases, as fewer bands are then necessary; here, P_{QFCC} is calculated up to 70 eV at 0.2 g/cm^3, up to 100 eV at 2.5 g/cm^3, and up to 200 eV at

20 g/cm^3. As a result of extensive tests of numerical convergence, the electronic pressures are obtained with an accuracy better than 0.1%.

As already found for boron [24] and lutetium [29], P_{OFWAA} is overall in better agreement with P_{QFCC} than P_{OFAA} because it includes the gradient correction to the local-density approximation of F_0. As temperature increases at given mass density, kinetic energy tends to prevail over potential energy so that the electronic density tends to get more homogeneous, thereby decreasing the impact of the local-density approximation of F_0. As a result, P_{QFCC} converges to P_{OFWAA} which, in its turn, converges to P_{OFAA}. As observed in Ref. [24], the convergence of P_{QFCC} to P_{OFWAA} is not monotonic but oscillatory due to shell effects. However, contrary to the case of boron, there is only one oscillation for deuterium. As mass density increases, the relative magnitude of this oscillation decreases from 7.3% at 0.2 g/cm^3 to 1.2% at 20 g/cm^3. This observation stems again from the fact that, as mass density increases, kinetic energy tends to prevail over potential energy. For the same reason, P_{OFAA} and P_{OFWAA} get closer overall when mass density increases. The temperature of convergence of the various electronic pressures to one another increases when mass density increases; for instance, the convergence of P_{QFCC} to P_{OFWAA} is obtained at about 50 eV at 0.2 g/cm^3, 100 eV at 2.5 g/cm^3, and 200 eV at 20 g/cm^3. As already found for boron [24] and lutetium [29], the proximity of P_{OFAA} and P_{OFWAA} is a good indicator of the proximity of P_{OFWAA} and P_{QFCC} at given mass density.

We now consider the domain $\rho \geqslant 20$ g/cm^3. At 20 g/cm^3, the maximal relative difference between P_{OFWAA} and P_{QFCC} in the domain $T \geqslant 1$ eV is only 1.2%. As observed in Fig. 1, this maximal relative difference decreases when mass density increases. Therefore, above 20 g/cm^3, it is possible to replace P_{QFCC} with P_{OFWAA} if one accepts a relative error less than 1.2%. Finally, in the domain 0.2–20 g/cm^3, it is possible to use P_{OFWAA} to extend P_{QFCC} at high temperature and, above 20 g/cm^3, it is possible to use P_{OFWAA} to reproduce P_{QFCC} on the whole domain $T \geqslant 1$ eV.

In Refs. [24] and [29], the nonrelativistic quantum versions of the all-electron average-atom models VAAQP [25–27] and INFERNO T [28] have been found useful to extend P_{QFCC} at high temperature in the cases of boron and lutetium. The subscripts VAAQP and INFERNO are used hereafter to designate the pressures of deuterium obtained with these two models and presented in Fig. 1. P_{INFERNO} is greater than P_{VAAQP} and P_{QFCC}. As temperature increases at given mass density, P_{VAAQP} and P_{INFERNO} converge to P_{QFCC} and to P_{OFWAA}; P_{VAAQP} converges to P_{QFCC} much faster than P_{INFERNO}. The temperature of convergence increases when mass density increases. As observed for P_{QFCC}, the convergence to P_{OFWAA} is oscillatory with only one oscillation whose relative magnitude decreases when mass density increases. P_{VAAQP} converges to P_{QFCC} before P_{QFCC} converges to P_{OFWAA}; it can therefore also be used to extend P_{QFCC} at high temperature below 20 g/cm^3. At 20 g/cm^3, the maximal relative difference between P_{QFCC} and P_{VAAQP} is 0.6% in the domain $T \geqslant 1$ eV; as this maximal relative difference decreases when mass density increases, it is possible to replace P_{QFCC} with P_{VAAQP} above 20 g/cm^3 if one accepts a relative error less than 0.6%.

The difference between the VAAQP, QFCC, and INFERNO models lies in the boundary conditions they use. QFCC is a rigorous periodic Wigner-Seitz (WS) cell model; it corresponds to the physical picture of an atom that is part of a fcc crystal. INFERNO is a spherical ion-in-cell plasma model in which an atom is viewed as a neutral WS sphere surrounded by a homogeneous electron gas neutralized by a uniform ion background. The idea of the spherical ion-in-cell model first appeared in the framework of the quasiclassical Thomas-Fermi model [48] as an approximation to the polyhedral WS cell of solid-state physics. In the framework of quantum mechanics, such a model includes an approximation on the equations of density-functional theory, which results in thermodynamic inconsistency. In the VAAQP model, the plasma free energy is approximated by using a first-order cluster expansion [50], which leads to the notion of an atom-in-plasma. The self-consistent field equations stem from a rigorous minimization of this plasma free energy under the constraint of overall charge neutrality. The model allows one to use rigorous thermodynamic definitions to calculate thermodynamic quantities, including pressure, and fulfills the virial theorem. A naive point of view would be that the INFERNO model is closer to a periodic cell model than VAAQP because it sticks in some way with the neutral WS cell hypothesis. The fact that P_{VAAQP} is generally closer to P_{QFCC} than P_{INFERNO} suggests, however, that the effect on pressure of the lack of thermodynamic consistency is larger than the effect of considering such different physical pictures as an atom in a crystal and an atom in a plasma.

In the rest of this work, the numerical results presented are obtained in the domain 0.2–20 g/cm^3. When necessary, the QFCC results are extended at high temperature with the OFWAA results; the notation QAA is henceforth used to designate QFCC extended with OFWAA.

B. Calculation of pressure and internal energy of deuterium

1. Ionic excess pressure

The two approaches OFMD and OFWMD do not implement a quantum treatment of $F_0[n(\mathbf{r})]$ contrary to QMD, which is thereby the reference to be reproduced. Comparing the electronic pressures P_{QFCC}, P_{OFAA}, and P_{OFWAA} amounts to comparing QMD, OFMD, and OFWMD applied to the calculation of the pressure obtained, in a single time step, with a fcc lattice of nuclei. As P_{OFWAA} is overall in better agreement with P_{QFCC} than P_{OFAA}, we now focus on the comparison of the total pressures P_{QMD} and P_{OFWMD}, respectively, obtained with QMD and OFWMD. As above, the LDA exchange-correlation functional is used.

In the limit of high temperature, the total pressure is expected to be the sum of the electronic pressure and of the kinetic pressure due to classical nuclei. The gap to this situation is measured by the ionic excess pressure that we define as

$$\delta P_{i,\alpha MD}(\rho,T) = P_{\alpha MD}(\rho,T) - P_{\alpha AA}(\rho,T) - P_{iK}(\rho,T), \quad (4)$$

where $\alpha = \text{Q}$ or OFW, and where P_{iK} is the kinetic pressure due to classical nuclei, that is $P_{iK} = \rho k T / m$, where k is the Boltzmann constant and m is the mass of an atom.

By construction, the ionic excess pressure characterizes the possibility of calculating an EOS with $P_{\alpha AA}$ and P_{iK} only, that is,
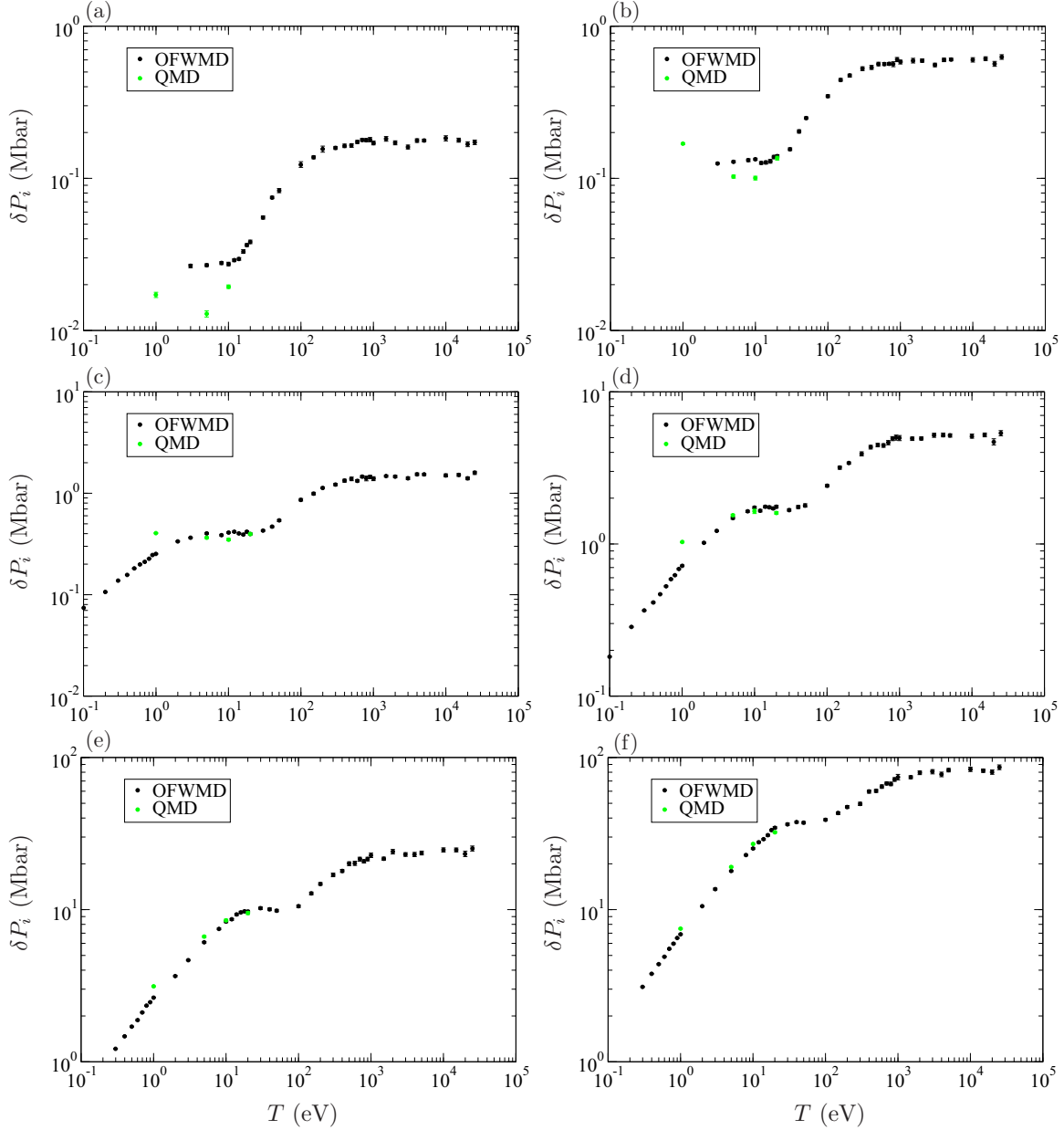
FIG. 2. Ionic excess pressure of deuterium, calculated with QMD or OFWMD, at the mass densities (a) 0.2 g/cm^3, (b) 0.5 g/cm^3, (c) 1 g/cm^3, (d) 2.5 g/cm^3, (e) 8 g/cm^3, and (f) 20 g/cm^3. The simulations have been performed with the LDA exchange-correlation functional.

without having to perform a molecular dynamics simulation. Another interest of this quantity is that the equality of $\delta P_{i,\mathrm{QMD}}$ and $\delta P_{i,\mathrm{OFWMD}}$ indicates that the difference $P_{\mathrm{QMD}} - P_{\mathrm{OFWMD}}$ is equal to the difference $P_{\mathrm{QAA}} - P_{\mathrm{OFWAA}}$; then, as P_{OFWMD}, P_{OFWAA}, and P_{QAA} can be calculated at high temperature, P_{QMD} can also be calculated at high temperature without proceeding to a direct QMD simulation. In this section we show that for deuterium above 0.2 g/cm^3, it is possible to carry out QMD calculations at sufficiently high temperature to observe the convergence of $\delta P_{i,\mathrm{QMD}}$ to $\delta P_{i,\mathrm{OFWMD}}$ so that, as explained above, the QMD results can be reproduced at high temperature.

The variation of $\delta P_{i,\mathrm{QMD}}$ and $\delta P_{i,\mathrm{OFWMD}}$ with temperature along various isochores in the domain 0.2–20 g/cm^3 is presented in Fig. 2. Below 1 g/cm^3, the change of curvature of $\delta P_{i,\mathrm{QMD}}(T)$ is connected to P_{QFCC} getting negative at 1 eV.

In the domain 0.5–20 g/cm^3, as temperature increases, the convergence of $\delta P_{i,\mathrm{QMD}}$ to $\delta P_{i,\mathrm{OFWMD}}$ occurs within statistical error at $T = 20$ eV or less. That this expected convergence can be observed within a statistical error that is small in relative terms (typically a few tenths of a percent of the total pressure) is an indication that, for both QMD and OFWMD, numerical convergence has been obtained properly. The variation of $\delta P_{i,\mathrm{QMD}}/P_{\mathrm{QMD}}$ with mass density along the isotherms 1, 5, 10, and 20 eV is presented in Fig. 3. It appears that at the thermodynamic conditions where $\delta P_{i,\mathrm{QMD}}$ gets close to $\delta P_{i,\mathrm{OFWMD}}$, the ionic excess pressure is at least an order of magnitude smaller than the total pressure; therefore comparing the ionic excess pressures $\delta P_{i,\mathrm{QMD}}$ and $\delta P_{i,\mathrm{OFWMD}}$ allows one to finely observe the convergence of P_{QMD} to $(P_{\mathrm{OFWMD}} - P_{\mathrm{OFWAA}} + P_{\mathrm{QAA}})$ as T increases at given ρ. Figure 3
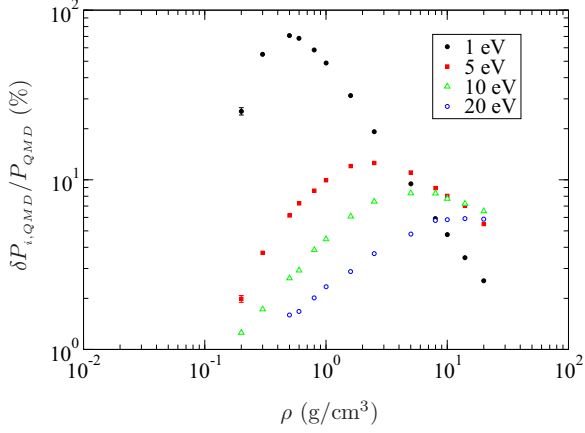
FIG. 3. Ratio of ionic excess pressure to total pressure of deuterium at $T = 1, 5, 10$, and 20 eV in the domain 0.2–20 g/cm^3. The simulations have been performed with QMD and the LDA exchange-correlation functional. The error bars are not displayed when they are smaller than the character size.

also shows that as mass density increases along an isotherm, $\delta P_{i,\mathrm{QMD}}/P_{\mathrm{QMD}}$ first increases then decreases; the maximum is obtained at a mass density that increases with temperature. Moreover, there are thermodynamic conditions in which the ionic excess pressure is small so that molecular dynamics is not necessary; this is the case above 10 eV at 0.2 g/cm^3, for instance, if one accepts to evaluate the total pressure with an accuracy of 1%.

At 0.2 g/cm^3, the highest temperature at which P_{QMD} has been calculated is 10 eV. Figure 2 shows that at this mass density and at $T = 10$ eV, $\delta P_{i,\mathrm{QMD}}$ and $\delta P_{i,\mathrm{OFWMD}}$ differ by a few standard deviations so that the convergence of $\delta P_{i,\mathrm{QMD}}$ to $\delta P_{i,\mathrm{OFWMD}}$ is not strictly obtained. At 20 eV, however, it can be considered as obtained, because as shown in Fig. 3 by extrapolation, above 10 eV at this mass density, the ionic excess pressure has a small relative contribution that decreases as temperature increases; as a result, replacing $\delta P_{i,\mathrm{QMD}}$ by $\delta P_{i,\mathrm{OFWMD}}$ has little influence on the result. Thus we will see later on that at 10 eV and 0.2 g/cm^3, replacing $\delta P_{i,\mathrm{QMD}}$ by $\delta P_{i,\mathrm{OFWMD}}$ in the calculation of P_{QMD} by Eq. (4) induces a relative difference of 0.5%; as the relative contribution of the ionic excess pressure decreases when temperature increases at 0.2 g/cm^3, this substitution will induce a still smaller relative difference at 20 eV. Finally, in the whole domain 0.2–20 g/cm^3, $\delta P_{i,\mathrm{QMD}}$ converges to $\delta P_{i,\mathrm{OFWMD}}$ at 20 eV or less.

We now consider the domain $\rho \geqslant 20$ g/cm^3. At 20 g/cm^3, the equality of $\delta P_{i,\mathrm{QMD}}$ and $\delta P_{i,\mathrm{OFWMD}}$ is verified within statistical error at 5, 10, and 20 eV. At 20 g/cm^3 and 1 eV, it appears in Fig. 3 that $\delta P_{i,\mathrm{QMD}}$ is less than 3% of P_{QMD} so that, again, replacing $\delta P_{i,\mathrm{QMD}}$ by $\delta P_{i,\mathrm{OFWMD}}$ has little influence on the value of P_{QMD}. We will see later on that at 20 g/cm^3 and 1 eV, the difference between $\delta P_{i,\mathrm{QMD}}$ and $\delta P_{i,\mathrm{OFWMD}}$ induces a relative difference of only 0.2% in the calculation of P_{QMD} by Eq. (4); as a result, we can regard $\delta P_{i,\mathrm{QMD}}$ and $\delta P_{i,\mathrm{OFWMD}}$ as equal in the whole range 1–20 eV. Since Fig. 2 shows that $\delta P_{i,\mathrm{QMD}}$ tends to $\delta P_{i,\mathrm{OFWMD}}$ as ρ increases at given T and as T increases at given ρ, the equality of $\delta P_{i,\mathrm{QMD}}$ and $\delta P_{i,\mathrm{OFWMD}}$ at 20 g/cm^3 in the domain 1–20 eV implies their equality in the domain $\rho \geqslant 20$

g/cm^3 and $T \geqslant 1$ eV. Finally, the convergence of $\delta P_{i,\mathrm{QMD}}$ to $\delta P_{i,\mathrm{OFWMD}}$ as temperature increases is observed in the whole domain $\rho \geqslant 0.2$ g/cm^3 and $T \geqslant 1$ eV.

2. Ionic internal energy

In order to obtain a complete EOS, one must also calculate the internal energy at given ρ and T. In this section, we show that as in the case of pressure, it is possible to reproduce the internal energy calculated by QMD at high temperature. The internal energies per atom are hereafter designated by the letter E, and the notations used are similar to those used for pressure. In order to compare internal energies regardless of the origin of energies, we consider a difference of energies and therefore define the ionic internal energy per atom $E_{i,\alpha MD}$ by

$$E_{i,\alpha MD}(\rho,T) = E_{\alpha MD}(\rho,T) - E_{\alpha AA}(\rho,T), \qquad (5)$$

where $\alpha = Q$, or OFW.

In this section, we show that as in the case of pressure, $E_{i,\mathrm{QMD}}$ converges to $E_{i,\mathrm{OFWMD}}$ as temperature increases at given mass density. This convergence is indeed observed in Fig. 4 at or below 20 eV in the domain 0.2–20 g/cm^3. As a result, as E_{OFWMD}, E_{OFWAA}, and E_{QAA} can be calculated at high temperature, E_{QMD} can be reproduced at high temperature in the domain 0.2–20 g/cm^3 by replacing $E_{i,\mathrm{QMD}}$ with $E_{i,\mathrm{OFWMD}}$ in Eq. (5). Figure 4 also shows that $E_{i,\mathrm{QMD}}/kT$ converges to $E_{i,\mathrm{OFWMD}}/kT$ as mass density increases at given temperature. With the axes chosen in Fig. 4, the curvature of the curves representing $E_{i,\mathrm{QMD}}/kT$ as a function of T changes below 1 g/cm^3. Note that a change of curvature of $\delta P_{i,\mathrm{QMD}}(T)$ has also been observed below 1 g/cm^3 in Fig. 2; again, this corresponds to P_{QFCC} getting negative at 1 eV. As expected, in the limit of high temperature, $E_{i,\mathrm{OFWMD}}$ tends to the internal energy per atom of a monatomic classical perfect gas, that is, $E_{iK} = 1.5kT$.

We now consider the domain $\rho \geqslant 20$ g/cm^3. $E_{i,\mathrm{QMD}}$ and $E_{i,\mathrm{OFWMD}}$ can be regarded as equal at 20 g/cm^3 in the range 1–20 eV; indeed, the variations of internal energy between consecutive states obtained in this domain with QMD and with OFWMD are equal within statistical error. Moreover, again in terms of variation with respect to T, $E_{i,\mathrm{QMD}}$ tends to $E_{i,\mathrm{OFWMD}}$ as ρ increases at given T and as T increases at given ρ; one interest of representing $E_{i,\alpha MD}/kT$ instead of $E_{i,\alpha MD}$ in Fig. 4 is to better illustrate this result. Consequently, as in the case of pressure, the equality of $E_{i,\mathrm{QMD}}$ and $E_{i,\mathrm{OFWMD}}$ at 20 g/cm^3 in the domain 1–20 eV implies their equality in the domain $T \geqslant 1$ eV and $\rho \geqslant 20$ g/cm^3. Finally, as in the case of pressure, the convergence of $E_{i,\mathrm{QMD}}$ to $E_{i,\mathrm{OFWMD}}$ as temperature increases is observed in the domain $\rho \geqslant 0.2$ g/cm^3 and $T \geqslant 1$ eV.

3. An extension of QMD at high temperature: OFWHMD

The convergence of $\delta P_{i,\mathrm{QMD}}$ to $\delta P_{i,\mathrm{OFWMD}}$ as T increases at given ρ is equivalent to the convergence of P_{QMD} to P_{OFWHMD}, defined by

$$P_{\mathrm{OFWHMD}}(\rho,T) = P_{\mathrm{OFWMD}}(\rho,T) - \delta P_e(\rho,T), \qquad (6)$$

$$\delta P_e(\rho,T) = P_{\mathrm{OFWAA}}(\rho,T) - P_{\mathrm{QAA}}(\rho,T), \qquad (7)$$

where the letter H in OFWHMD stands for hybrid as both the orbital-free and quantum approaches are involved in the
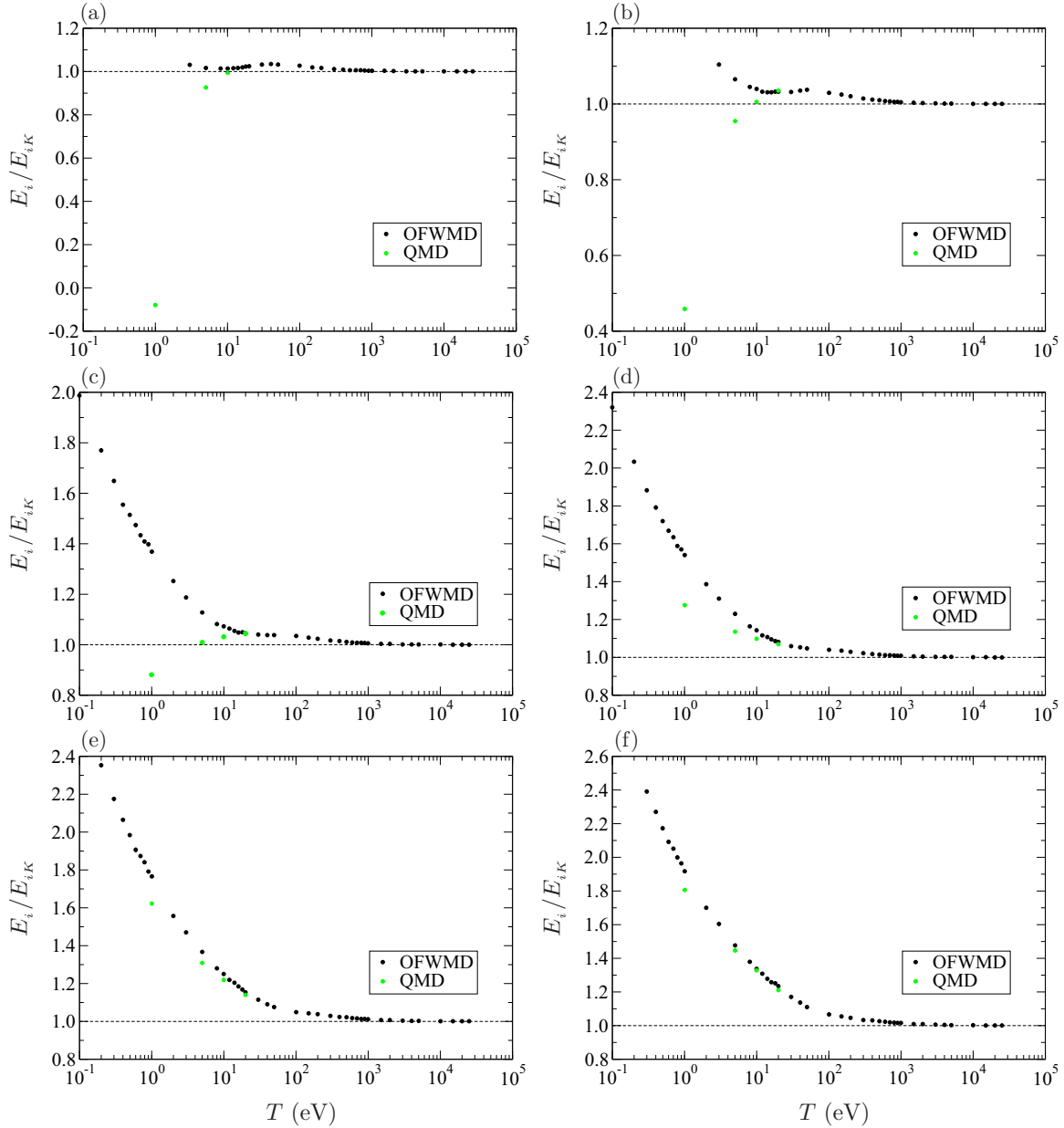
FIG. 4. Ratio of the ionic internal energy per atom of deuterium, calculated with QMD or OFWMD, to $E_{iK} = 1.5kT$ at the mass densities (a) 0.2 g/cm^3, (b) 0.5 g/cm^3, (c) 1 g/cm^3, (d) 2.5 g/cm^3, (e) 8 g/cm^3, and (f) 20 g/cm^3. k designates the Boltzmann constant. The simulations have been performed with the LDA exchange-correlation functional.

definition. Like P_{OFWMD}, P_{OFWAA}, and P_{QAA}, P_{OFWHMD} can be calculated at high temperature. The convergence of $E_{i,\mathrm{QMD}}$ to $E_{i,\mathrm{OFWMD}}$ discussed above is equivalent to the convergence of E_{QMD} to E_{OFWHMD}, with E_{OFWHMD} defined similarly to P_{OFWHMD}. In view of their definitions, P_{OFWHMD} and E_{OFWHMD} verify thermodynamic self-consistence.

In Refs. [24] and [29], defining P_{OFWHMD} has allowed us to observe a monotonic convergence of P_{QMD} to P_{OFWHMD} for boron and lutetium as T increases at given ρ. We show that this is also the case here for deuterium, as illustrated in Table I and in Fig. 5; no orbital-free simulation has been performed below 3 eV and 0.8 g/cm^3 because the gradient correction gets so large that the orbital-free approach, that treats the inhomogeneity of the electronic density approximately, is no

longer meaningful. As a result of the monotonic convergence, P_{QMD} converges faster to P_{OFWHMD} than to P_{OFWMD} (to which the convergence of P_{QMD} is oscillatory); this result appears more clearly at low density, for instance in Table I at 0.5 g/cm^3. As noted in Sec. B 1, Table I indicates that P_{QMD} and P_{OFWHMD} differ by 0.5% at 0.2 g/cm^3 and 10 eV and by 0.2% at 20 g/cm^3 and 1 eV.

4. A reproduction of QMD at any temperature: QOFWH

We have defined the OFWHMD pressure and internal energy that reproduce the QMD results at any temperature greater than 20 eV in the domain $\rho \geqslant 0.2$ g/cm^3 for deuterium. Below 20 eV, QMD simulations are available. It is therefore possible to reproduce the QMD

TABLE I. Total pressure of deuterium calculated with OFWMD, OFWHMD, and QMD. The standard deviations are indicated in parentheses. The simulations have been performed with the LDA exchange correlation. No OFWMD simulation has been performed at 1 eV below 0.8 g/cm^3 because the gradient correction gets so large that orbital-free simulations, that treat the inhomogeneity of the electronic density approximately, are no longer meaningful.

		Total pressure (Mbar)					
ρ (g/cm^3)	T (eV)	OFWMD		OFWHMD		QMD	
0.2	1					0.0676	(6.8[−4])
	5	0.6671	(5.6[−4])	0.6609	(5.6[−4])	0.6468	(5.9[−4])
	10	1.5153	(7.3[−4])	1.5540	(7.3[−4])	1.5460	(5.0[−4])
	20	3.405	(1.0[−3])	3.460	(1.0[−3])		
	30	5.375	(1.3[−3])	5.393	(1.3[−3])		
	40	7.322	(1.4[−3])	7.331	(1.4[−3])		
	50	9.251	(2.6[−3])	9.256	(2.6[−3])		
	100	18.879	(5.3[−3])	18.879	(5.3[−3])		
0.3	1					0.1094	(9.7[−4])
	5	1.006	(1.2[−3])	0.990	(1.2[−3])	0.975	(1.2[−3])
	10	2.261	(1.2[−3])	2.311	(1.2[−3])	2.297	(1.1[−3])
	20	5.050	(1.3[−3])	5.140	(1.3[−3])		
	30	7.987	(2.0[−3])	8.026	(2.0[−3])		
	40	10.907	(2.4[−3])	10.926	(2.4[−3])		
	50	13.812	(3.7[−3])	13.824	(3.7[−3])		
	100	28.256	(4.1[−3])	28.256	(4.1[-3])		
0.5	1					0.238	(2.4[−3])
	5	1.736	(2.0[−3])	1.692	(2.0[−3])	1.666	(2.4[−3])
	10	3.785	(2.2[−3])	3.851	(2.2[−3])	3.818	(2.8[−3])
	20	8.333	(2.8[−3])	8.492	(2.8[−3])	8.487	(3.9[−3])
	30	13.151	(3.2[−3])	13.251	(3.2[−3])		
	40	18.023	(5.1[−3])	18.071	(5.1[−3])		
	50	22.868	(4.7[−3])	22.898	(4.7[−3])		
	100	46.924	(7.2[-3])	46.934	(7.2[−3])		
0.8	1					0.540	(3.4[−3])
	5	2.949	(4.8[−3])	2.848	(4.8[−3])	2.816	(5.1[−3])
	10	6.160	(5.6[−3])	6.234	(5.6[−3])	6.181	(5.8[−3])
	20	13.281	(5.2[−3])	13.534	(5.2[−3])	13.521	(7.9[−3])
	30	20.862	(6.8[−3])	21.074	(6.8[−3])		
	40	28.620	(8.4[−3])	28.731	(8.4[−3])		
	50	36.365	(8.4[−3])	36.436	(8.4[−3])		
	100	74.84	(1.1[−2])	74.86	(1.1[−2])		
1	1	1.090	(2.4[−3])	0.679	(2.4[−3])	0.830	(3.9[−3])
	5	3.858	(7.6[−3])	3.711	(7.6[−3])	3.673	(7.2[−3])
	10	7.805	(6.8[−3])	7.877	(6.8[−3])	7.816	(9.3[−3])
	20	16.611	(8.5[−3])	16.923	(8.5[−3])	16.92	(9.9[−3])
	30	26.031	(7.6[−3])	26.323	(7.6[−3])		
	40	35.661	(8.8[−3])	35.832	(8.8[−3])		
	50	45.31	(1.3[−2])	45.42	(1.3[−2])		
	100	93.49	(2.5[−2])	93.52	(2.5[−2])		
1.6	1	2.573	(4.5[−3])	1.931	(4.5[−3])	2.167	(5.9[−3])
	5	6.97	(1.4[−2])	6.66	(1.4[−2])	6.66	(1.7[-2])
	10	13.10	(1.3[−2])	13.14	(1.3[−2])	13.09	(1.6[−2])
	20	26.87	(1.7[−2])	27.33	(1.7[−2])	27.27	(1.4[−2])
	30	41.60	(1.7[−2])	42.13	(1.7[−2])		
	40	56.85	(1.7[−2])	57.24	(1.7[−2])		
	50	72.20	(2.0[−2])	72.45	(2.0[−2])		
	100	149.12	(3.6[−2])	149.20	(3.6[−2])		
2.5	1	5.974	(7.4[−3])	5.046	(7.4[−3])	5.354	(9.4[−3])
	5	12.79	(2.2[−2])	12.23	(2.2[−2])	12.30	(2.5[−2])
	10	22.19	(3.2[−2])	22.12	(3.2[−2])	22.03	(5.5[−2])
	20	43.08	(3.9[−2])	43.71	(3.9[−2])	43.56	(3.1[−2])
	30	65.53	(3.2[−2])	66.40	(3.2[−2])		

TABLE I. (*Continued.*)

ρ (g/cm^3)	T (eV)	Total pressure (Mbar)					
		OFWMD		OFWHMD		QMD	
	40	88.96	(4.1[−2])	89.71	(4.1[−2])		
	50	112.69	(4.5[−2])	113.24	(4.5[−2])		
	100	232.38	(4.8[−2])	232.55	(4.8[−2])		
5	1	22.45	(1.7[−2])	20.93	(1.7[−2])	21.40	(1.8[−2])
	5	35.80	(5.1[−2])	34.62	(5.1[−2])	34.94	(5.1[−2])
	10	53.64	(8.3[−2])	53.15	(8.3[−2])	53.10	(8.1[−2])
	20	93.21	(7.8[−2])	94.04	(7.8[−2])	93.69	(7.8[−2])
	30	136.28	(8.2[−2])	137.87	(8.2[−2])		
	40	181.60	(8.4[−2])	183.38	(8.4[−2])		
	50	227.7	(1.1[−1])	229.3	(1.1[−1])		
	100	464.5	(1.2[−1])	465.2	(1.2[−1])		
8	1	54.61	(2.0[−2])	52.57	(2.0[−2])	53.06	(2.3[−2])
	5	75.55	(7.1[−2])	73.84	(7.1[−2])	74.38	(9.1[−2])
	10	103.3	(1.2[−1])	102.3	(1.2[−1])	102.5	(1.3[−1])
	20	164.1	(1.9[−1])	164.8	(1.9[−1])	164.6	(2.1[−1])
	30	230.7	(1.9[−1])	232.8	(1.9[−1])		
	40	300.4	(2.0[−1])	303.2	(2.0[−1])		
	50	372.4	(1.8[−1])	375.3	(1.8[−1])		
	100	746.7	(2.1[−1])	748.1	(2.1[−1])		
10	1	82.85	(2.9[−2])	80.55	(2.9[−2])	81.05	(2.7[−2])
	5	108.7	(1.2[−1])	106.7	(1.2[−1])	107.6	(1.0[−1])
	10	142.6	(1.7[−1])	141.4	(1.7[−1])	141.7	(1.8[−1])
	20	217.1	(2.2[−1])	217.7	(2.2[−1])	217.4	(2.4[−1])
	30	298.0	(2.2[−1])	300.4	(2.2[−1])		
	40	384.5	(2.6[−1])	387.8	(2.6[−1])		
	50	473.7	(2.6[−1])	477.3	(2.6[−1])		
	100	936.8	(2.4[−1])	938.9	(2.4[−1])		
14	1	154.34	(4.3[−2])	151.63	(4.3[−2])	152.27	(5.5[−2])
	5	191.3	(1.2[−1])	188.8	(1.2[−1])	190.1	(1.5[−1])
	10	237.1	(2.3[−1])	235.3	(2.3[−1])	236.1	(2.3[−1])
	20	338.0	(3.2[−1])	338.3	(3.2[−1])	337.5	(3.0[−1])
	30	449.1	(4.0[−1])	451.6	(4.0[−1])		
	40	564.8	(5.0[−1])	568.9	(5.0[−1])		
	50	686.2	(3.7[−1])	691.2	(3.7[−1])		
	100	1325.2	(5.0[−1])	1328.9	(5.0[−1])		
20	1	296.87	(5.5[−2])	293.72	(5.5[−2])	294.35	(6.7[−2])
	5	349.3	(1.8[−1])	346.4	(1.8[−1])	347.5	(2.0[−1])
	10	413.8	(3.1[−1])	411.6	(3.1[−1])	413.4	(3.7[−1])
	20	554.2	(5.7[−1])	554.0	(5.7[−1])	551.7	(5.1[−1])
	30	703.8	(6.4[−1])	706.2	(6.4[−1])		
	40	864.3	(5.8[−1])	869.0	(5.8[−1])		
	50	1031.1	(6.6[−1])	1037.6	(6.6[−1])		
	100	1927.9	(6.6[−1])	1934.4	(6.6[−1])		

EOS of deuterium at any temperature in the domain 0.2–20 g/cm^3 with OFWHMD results above 20 eV and QMD results below 20 eV.

We now define the QOFWH EOS as that constructed with QMD at low temperature (when necessary) and OFWHMD beyond the temperature of convergence of QMD to OFWHMD. In other words,

$$X_{\mathrm{QOFWH}}(\rho,T) = \begin{cases} X_{\mathrm{QMD}}(\rho,T); & T \leqslant T_H(\rho) \\ X_{\mathrm{OFWHMD}}(\rho,T); & T \geqslant T_H(\rho), \end{cases} \quad (8)$$

where $X = P$ or E, depending on whether it represents pressure or internal energy per atom, and $T_H(\rho)$ is a temperature where QMD has converged to OFWHMD at mass density ρ. In the present case, as discussed above, it is possible to take $T_H(\rho) = 20$ eV in the domain 0.2–20 g/cm^3 and $T_H(\rho) = 1$ eV in the domain $\rho \geqslant 20$ g/cm^3. When $T_H(\rho) = 1$ eV, no QMD results are necessary for the domain $T \geqslant 1$ eV considered in the present work, of course.

QOFWH reproduces the EOS of deuterium obtained with QMD in the domain $T \geqslant 1$ eV and $\rho \geqslant 0.2$ g/cm^3 (with the
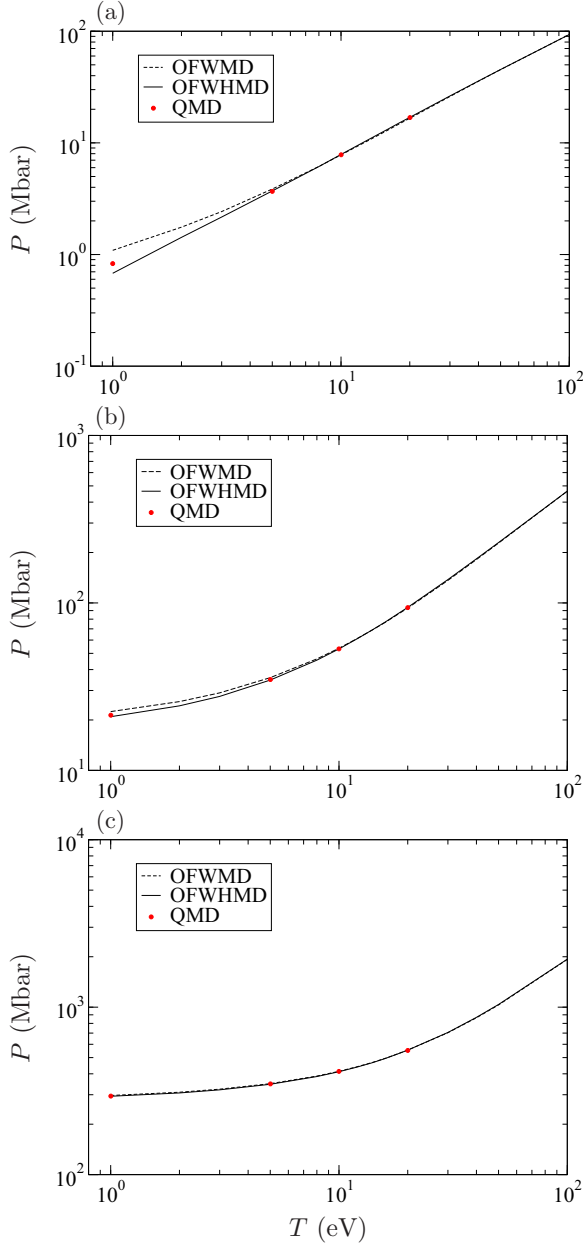
FIG. 5. Total pressure of deuterium calculated with OFWMD, OFWHMD, and QMD at (a) 1 g/cm^3, (b) 5 g/cm^3, and (c) 20 g/cm^3. The simulations have been performed with the LDA exchange-correlation functional.

exception of the subdomain where the system is in a solid phase not addressed in the present work). The results obtained for deuterium can be used for hydrogen and tritium by applying the mass density scaling described in Ref. [15]. We emphasize that QOFWH is not an *ad hoc* construction smoothly connecting two approaches and that it reproduces the QMD results within statistical error in the thermodynamic domain considered. Indeed, we know that $\delta P_{i,\text{QMD}}$ has to eventually converge to $\delta P_{i,\text{OFWMD}}$ as temperature increases at given mass density and that, in the thermodynamic domain addressed, we can calculate $\delta P_{i,\text{QMD}}$ at sufficiently high temperature to observe this convergence. As a result, beyond the temperature of convergence $T_H(\rho)$, $\delta P_{i,\text{QMD}}$ is known as equal to $\delta P_{i,\text{OFWMD}}$,

which can be calculated at any high temperature; since, as discussed in Sec. III A, P_{QAA} can be calculated at any temperature, P_{QMD} can be calculated above $T_H(\rho)$ through Eq. (4). Below $T_H(\rho)$, P_{QMD} can be calculated directly.

C. Sensitivity of QOFWH to electron exchange correlation

The choice of an approximation for the electron exchange-correlation functional F_{xc} is the only degree of freedom in QOFWH calculations. In this section, we investigate the sensitivity of QOFWH to this functional in the domain 0.2–20 g/cm^3 and $T \geqslant 1$ eV. The LDA exchange correlation has been used so far. Another kind of widely used functional is the generalized gradient approximation (GGA) [51] that has been found to give a better description of the EOS of solid hydrogen than LDA [15]. GGA corrects LDA with a function of both $n(\mathbf{r})$ and $\nabla n(\mathbf{r})$; in the limit of a homogeneous gas of electrons, GGA and LDA are identical. GGA and LDA have been constructed for ground-state calculations and therefore do not depend on temperature. Ichimaru *et al.* have proposed an electron exchange-correlation functional depending on temperature in Eq. (3.83) of Ref. [52]; as it is based on a local-density approximation, we designate it by the subscript LDAT.

As noted in Ref. [24], the ionic excess pressure is little sensitive to the choice of the exchange-correlation functional. Writing the invariance of the ionic excess pressure by interchange of GGA and LDA amounts to writing

$$P_{\text{QOFWH-GGA}}(\rho,T) = P_{\text{QOFWH-LDA}}(\rho,T) + P_{\text{QAA-GGA}}(\rho,T)$$
$$- P_{\text{QAA-LDA}}(\rho,T), \qquad (9)$$

where the subscripts GGA and LDA, respectively, designate the pressures obtained with GGA and LDA. As the computations with GGA are significantly more costly than those with LDA, we have calculated $P_{\text{QOFWH-GGA}}$ with Eq. (9) after verifying it in conditions where LDA and GGA differ most. A similar equation applies to the internal energy per atom obtained with GGA.

LDAT has not been implemented with QMD in ABINIT. Incidentally, the use of LDAT with QMD would considerably increase computation times. As in the case of GGA, the invariance of the ionic excess pressure allows one to write Eq. (9) with GGA replaced by LDAT. As LDAT gives only a small perturbation of LDA for the EOS [40], we have chosen to approximate $P_{\text{QAA-LDAT}} - P_{\text{QAA-LDA}}$ by $P_{\text{OFWAA-LDAT}} - P_{\text{OFWAA-LDA}}$. Finally, we approximate the QOFWH pressure obtained with LDAT by

$$P_{\text{QOFWH-LDAT}}(\rho,T) = P_{\text{QOFWH-LDA}}(\rho,T) + P_{\text{OFWAA-LDAT}}(\rho,T)$$
$$- P_{\text{OFWAA-LDA}}(\rho,T), \qquad (10)$$

with a similar equation applying to the internal energy per atom.

LDAT corrects LDA in order to take into account the influence of temperature in F_{xc}, and GGA corrects LDA in order to take into account the influence of the nonhomogeneity of $n(\mathbf{r})$ in F_{xc}. In an attempt to take into account both temperature and the nonhomogeneity of $n(\mathbf{r})$, we now define the pressure designated by the subscript GGAT by

$$P_{\text{QOFWH-GGAT}}(\rho,T) = P_{\text{QOFWH-GGA}}(\rho,T) + P_{\text{OFWAA-LDAT}}(\rho,T)$$
$$- P_{\text{OFWAA-LDA}}(\rho,T), \qquad (11)$$
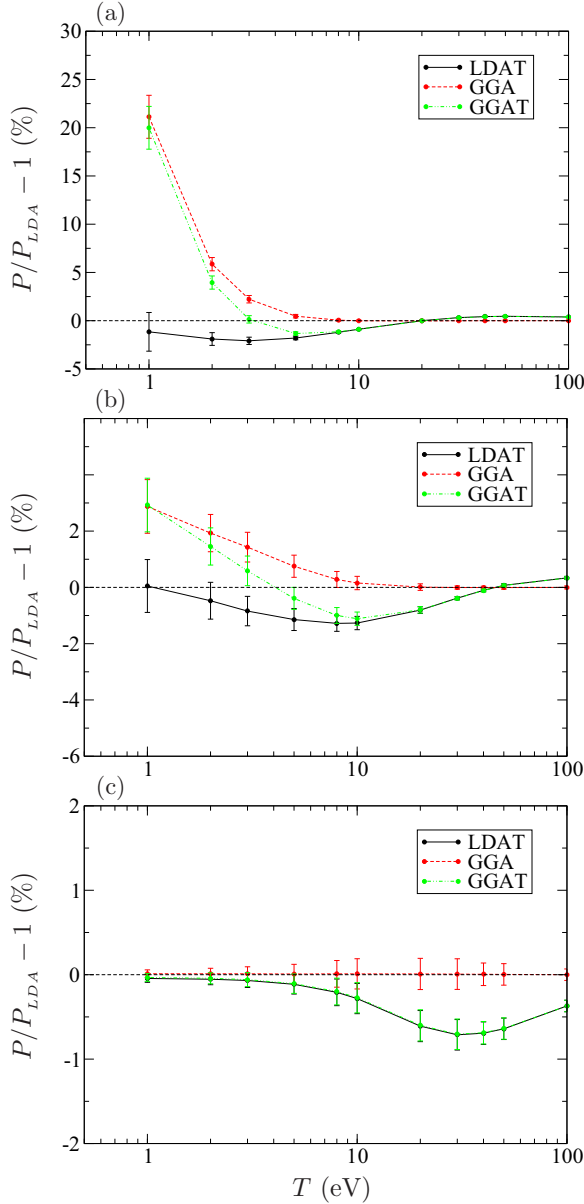
FIG. 6. Sensitivity of the pressure of deuterium calculated with QOFWH to exchange correlation at (a) 0.2 g/cm^3, (b) 1 g/cm^3, and (c) 20 g/cm^3. The pressure calculated with the LDA exchange-correlation functional is chosen as the reference. In (c), the curves GGAT and LDAT are superimposed.

with a similar equation applying to the internal energy per atom. This definition of GGAT amounts to assuming that the small influence of T in F_{xc} is the same on total pressure and internal energy whether or not the nonhomogeneity of $n(\mathbf{r})$ is taken into account in F_{xc}.

The sensitivity of the QOFWH pressure of deuterium to exchange correlation is presented in Fig. 6, where the pressure calculated with LDA is taken as the reference, at $\rho = 0.2$, 1, and 20 g/cm^3. It appears that using GGA instead of LDA increases pressure, up to 21% at 1 eV and 0.2 g/cm^3. Moreover, the relative difference between GGA and LDA decreases when T increases at given ρ, and when ρ increases at given T; as

T or ρ increases, kinetic energy tends to prevail over potential energy so that electronic density tends to get homogeneous and GGA tends to LDA. Above 10 eV, GGA does not differ from LDA (within statistical error) in the domain $\rho \geqslant 0.2$ g/cm^3. We have also found that, above 2.5 g/cm^3, GGA does not differ from LDA in the domain $T \geqslant 1$ eV.

Using LDAT instead of LDA mainly decreases pressure. The pressures obtained with LDAT and LDA are equal within statistical error at low temperature, where they are close by construction, and are close at high temperature where kinetic energy prevails over exchange correlation. At 100 eV, the pressures obtained with LDA and LDAT differ by less than 0.5%. The largest relative difference between LDA and LDAT along an isochore is 2% at 0.2 g/cm^3 and 3 eV. It decreases when mass density increases because kinetic energy tends to further prevail over exchange correlation; it is 0.7% at 20 g/cm^3 and 30 eV. The temperature at which the largest relative difference between LDA and LDAT is obtained along an isochore increases when mass density increases because T intervenes in the LDAT exchange-correlation functional through its ratio to the Fermi temperature [52].

The GGAT results include the influence of temperature, which decreases pressure, and of the gradient correction that increases pressure. As temperature increases at given mass density, the relative difference between the GGAT and LDA pressures decreases in algebraic value, reaches a minimum, then increases to tend to 0. Above a temperature depending on mass density, the gradient correction is negligible so that the GGAT pressures are equal to the LDAT pressures. At 0.2 g/cm^3 and 1 g/cm^3, the influence of the gradient correction prevails up to 2 eV; at 20 g/cm^3, there is no more influence of the gradient correction so that the GGAT pressures are equal to the LDAT pressures on the whole domain of temperature considered.

IV. COMPARISON TO OTHER APPROACHES

In this section, we compare QOFWH to various approaches in the literature. The EOS of deuterium or hydrogen has been addressed in particular with PIMC [1], QMD [10,14], an association of QMD and PIMC [15], and a chemical model proposed by Kerley [53] and designated by Kerley03 in Ref. [1]. Hu *et al.* [1] have applied PIMC to deuterium and have produced many data in the domain 0.002–1596 g/cm^3 and 1.35–5500 eV. QOFWH and QMD assume a classical ionic behavior, whereas PIMC takes the quantum effects into account for both electrons and ions; as a result, PIMC needs no approximation of exchange correlation. However, PIMC cannot be applied at low temperature, typically below one-tenth of the Fermi temperature [1]. QMD, implemented with GGA, has been applied to hydrogen in the domain (0.043–1.7 eV, 0.5–5 g/cm^3) by Holst *et al.* [14] and to deuterium in the domain (0.17–2.7 eV, 0.506–0.851 g/cm^3) by Lenosky *et al.* [10]. The difficulty of addressing high temperatures with QMD and low temperatures with PIMC has led Caillabet *et al.* [15] to combine data obtained with both methods to construct a fit giving the EOS of a fluid phase of hydrogen in the domain 0.2–5 g/cm^3 and $T \leqslant 10$ eV.

In this section, we implement QOFWH with GGAT; the GGAT subscript is omitted in the rest of this work. The

QMD data of Refs. [10] and [14] are obtained with GGA. As GGAT coincides with GGA within statistical error at the low temperatures at which the QMD data of Refs. [10] and [14] are produced, the choice of GGAT in the implementation of QOFWH allows a comparison with these QMD results. The fit of the QMD results obtained for hydrogen by Holst *et al.* [14] is used to get QMD data for deuterium through the mass density scaling described in Ref. [15]. Moreover, by using the evaluation of Caillabet *et al.* [15], we have verified that the quantum correction to classical ionic behavior for the pressure of hydrogen is less than 0.1% in the domain $T \geqslant 1$ eV and 0.2–5 g/cm^3. As a result, we can also apply the mass density scaling to the fit of Caillabet *et al.*, proposed for hydrogen, to get EOS data for deuterium [15].

A. Isochores

We compare QOFWH to the results of Refs. [1,14,15,53] along some isochores calculated in Ref. [1] in the domain 0.2–15.7 g/cm^3. The results of Lenosky *et al.* [10] are not considered here because they are obtained in a limited range of mass density. The QOFWH pressures are obtained by interpolating from a table calculated at thermodynamic conditions that do not coincide in general with those of Ref. [1]. At given ρ and T, a first quadratic interpolation is used to calculate pressure at ρ at the tabulated temperatures, then a second quadratic interpolation is used to calculate pressure at ρ and T. The interpolation error is evaluated by comparing the pressures obtained to those given by linear interpolations; the
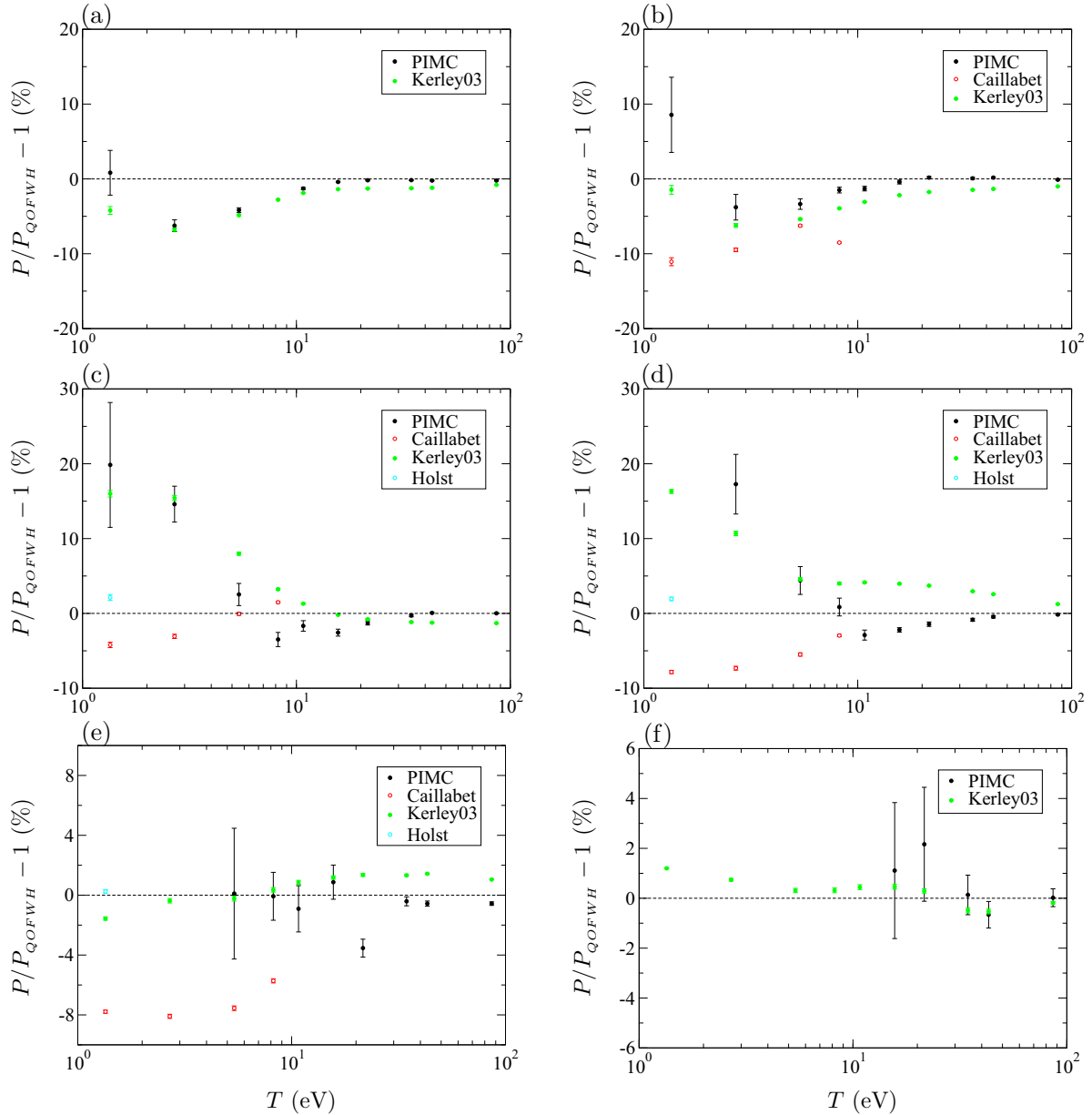
FIG. 7. Comparison of the pressure of deuterium calculated with various approaches along the isochores (a) 0.199 561 g/cm^3, (b) 0.389 768 g/cm^3, (c) 1.156 88 g/cm^3, (d) 1.963 61 g/cm^3, (e) 4.048 19 g/cm^3, and (f) 15.708 9 g/cm^3. The approaches considered are designated as follows: PIMC [1], Caillabet [15], Kerley03 [53], and Holst [14]. QOFWH implemented with the GGAT exchange-correlation functional is taken as the reference.

relative difference between them, that we regard as an upper bound of the interpolation error, is less than 1% at all the conditions considered.

The results are presented in Fig. 7. At 1.35 eV (15 625 K) and at the mass densities considered, QOFWH is based on direct QMD calculations. Figures 7(c)–7(e) show that our QMD results agree with the fit of Holst *et al.* [14] that reproduces their own QMD results within 5%. For the most part, the Caillabet pressures differ from the QOFWH pressures by 5%–11% at the mass densities considered; this is so even at 4.048 19 g/cm^3 [Fig. 7(e)] where all the other approaches are in good agreement. The relative difference between Caillabet and PIMC reaches up to 24% (6 standard deviations) at 1.963 61 g/cm^3 [Fig. 7(d)] and 2.69 eV (31 250 K); this result is surprising in view of the fact that the fit of Caillabet *et al.* is constructed, above 1 eV, from PIMC results [15]. At and above 4.048 19 g/cm^3 [Figs. 7(e) and 7(f)], Kerley03 remains within 2% of QOFWH in the temperature range considered; at and below 1.963 61 g/cm^3 [Figs. 7(a)–7(d)], the relative difference between Kerley03 and QOFWH can reach 16% at 1.35 eV (15 625 K), mainly decreases as temperature increases, and is 1% or less at 86.2 eV (10^6 K).

We now compare QOFWH and PIMC. In the PIMC approach, the statistical error increases as mass density increases at a given temperature [1]; when unusually large (say, more than 2%) statistical errors occur in Fig. 7, they come mainly from PIMC. As already noted by Driver and Militzer [22], a difference between QMD, or equivalently QOFWH, and PIMC comes from a numerical problem in the implementation of PIMC or from the choice of the exchange-correlation functional used with QMD. In the case of neon, Driver and Militzer [22] also evoke a possible insufficiency of the pseudopotential; we rule out this problem here because all numerical parameters, including those connected to the pseudopotential, have been chosen to ensure numerical convergence of pressure and internal energy within statistical error.

Above 10 eV, QOFWH and PIMC agree within 2.5% or within statistical error at all mass densities [except 3.5% for the result at 21.5 eV and 4.048 19 g/cm^3, which appears atypical in Fig. 7(e)]; this induces us to think that, in this domain of temperature, GGAT, or equivalently in practice LDAT, is a good approximation of exchange correlation and that both QOFWH and PIMC give reliable results. It can be noted that the use of GGAT instead of GGA in the domain $T \geqslant 10$ eV generally reduces the relative difference between PIMC and QOFWH; however, the relative difference between GGA and GGAT is less than 1.5% in this domain.

Between 5 and 10 eV, the relative difference between PIMC and QOFWH is less than 5%. Below 5 eV, as mass density increases at a given temperature, the relative difference between PIMC and QOFWH increases (in algebraic value) until the temperature can no longer be calculated in PIMC; this relative difference is 20% at 1.35 eV (15 625 K) and 1.156 88 g/cm^3 [Fig. 7(c)] and 17% at 2.69 eV (31 250 K) and 1.963 61 g/cm^3 [Fig. 7(d)]. At the same time, the statistical error on the relative difference increases to unusually large values because of PIMC. As already indicated, a difference between PIMC and QOFWH comes from a numerical problem in PIMC or from the choice of F_{xc}. There is no method to test the exactness of F_{xc}. It can nevertheless be observed that,
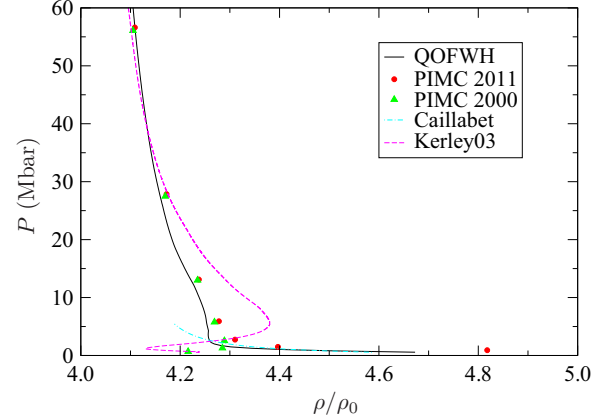
FIG. 8. Hugoniot of deuterium, calculated with the initial conditions $\rho_0 = 0.171$ g/cm^3 and $E_0 = -15.886$ eV/at, in the domain $T \geqslant 1$ eV and $P \leqslant 60$ Mbar. The approaches considered are designated as follows: PIMC2011 [1], PIMC2000 [7], Caillabet [15], and Kerley03 [53]. Our approach, QOFWH, is implemented with the GGAT exchange-correlation functional.

below 3 eV at 1.156 88 g/cm^3 or 1.963 61 g/cm^3 [Figs. 7(c) or 7(d)] where the largest relative differences occur, the QOFWH pressures are not very sensitive to the interchange of the exchange-correlation functionals; indeed, as illustrated in Fig. 6, the effect of interchanging LDA and GGA (or LDAT and GGAT) is 3% at 1 g/cm^3 and 1 eV and decreases when mass density or temperature increases. The fact that large relative differences between PIMC and QOFWH occur in conditions where PIMC has large statistical errors and where QOFWH is not very sensitive to the interchange of LDA and GGA suggests that it might be useful to revisit PIMC calculations at these conditions.

B. Hugoniot

We now compare the Hugoniot of deuterium calculated with QOFWH implemented with GGAT to the Hugoniot curves calculated with PIMC [1,7], the fit of Caillabet *et al.* [15], the fit of Lenosky *et al.* [10], and Kerley03 [53]. All Hugoniot curves are obtained with an initial state characterized by a mass density $\rho_0 = 0.171$ g/cm^3, zero pressure, and an internal energy $E_0 = -15.886$ eV/at [7]. (In the case of Lenosky *et al.*, E_0 is not necessary as the fit is constructed to reproduce $E - E_0$ [10].) They are presented in Figs. 8 and 9. As the fit of Lenosky *et al.* is applicable on a limited domain of temperature ($T \leqslant 2.7$ eV) [10], it is represented only in Fig. 9 that shows a smaller domain of the Hugoniot. For PIMC2000, we have reported the Hugoniot calculations of Ref. [7]. For PIMC2011, the Hugoniot equation has been solved by interpolation of the results of Ref. [1] obtained along isochores. The same interpolation method as that described in Sec. IV A has been used to obtain the curves PIMC2011 and QOFWH. The Caillabet results slightly differ from the Hugoniot of Ref. [15]; we attribute this to a different choice for the internal energy of the initial state. The Hugoniot curves of deuterium usually presented have a maximum compression ratio; here, except for Kerley03, no maximum compression ratio appears because only the domain $T \geqslant 1$ eV is presented.
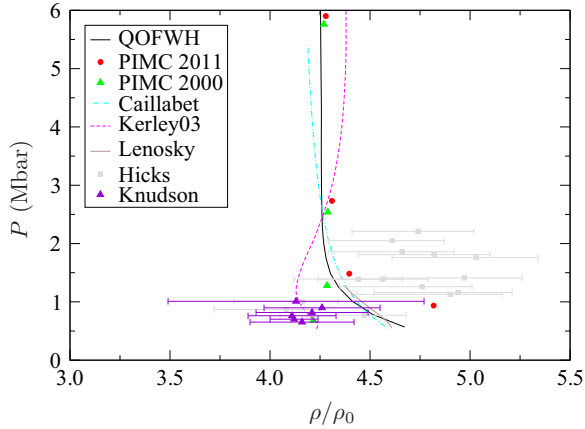
FIG. 9. Hugoniot of deuterium, calculated with the initial conditions $\rho_0 = 0.171 \, \text{g/cm}^3$ and $E_0 = -15.886 \, \text{eV/at}$, in the domain $T \geqslant 1 \, \text{eV}$ and $P \leqslant 6 \, \text{Mbar}$. The approaches considered are designated as follows: PIMC2011 [1], PIMC2000 [7], Caillabet [15], Lenosky [10], and Kerley03 [53]. Our approach, QOFWH, is implemented with the GGAT exchange-correlation functional. The experimental results found in Refs. [54] and [55] are respectively designated Knudson and Hicks.

It appears in Fig. 8 that Kerley03 tends to PIMC and QOFWH at high pressure. In the domain of low pressure considered in Fig. 9, the two curves obtained with PIMC are very different according to whether they are based on the results of Ref. [7] or on the results of Ref. [1]. Figures 8 and 9 show that, as pressure (or temperature) increases, the two PIMC curves tend to each other and to QOFWH; indeed, we have seen in Sec. IV A that, along isochores, PIMC is close to QOFWH at high temperature. Figure 9 also presents experimental results [54,55] above 0.5 Mbar (so that $T \geqslant 1 \, \text{eV}$). QOFWH and the other approaches considered in Fig. 9 give Hugoniot curves that agree with the experimental results within the very large experimental error bars.

V. CONCLUSION

We have constructed a first-principles EOS of deuterium, based on DFT-MD, reproducing the QMD results in the domain $T \geqslant 1 \, \text{eV}$ and $\rho \geqslant 0.2 \, \text{g/cm}^3$ (calculations performed in practice up to $25\,000 \, \text{eV}$ and $20\,000 \, \text{g/cm}^3$). Apart from shell effects that can be accounted for by using a fcc lattice of ions, orbital-free molecular dynamics simulations are a natural limit of QMD simulations as temperature and/or mass density increase. The QMD simulations have been performed at sufficiently high temperature and with a careful study of numerical convergence to observe that this limit is indeed obtained within statistical error. As a result, by using orbital-free simulations, the EOS constructed smoothly and consistently reproduces the QMD results up to any high temperature. Contrary to PIMC at temperatures of the order of 0.1 Fermi temperature, this EOS is not affected by large

statistical errors in the thermodynamic domain considered. This *ab initio* approach allows one to consistently cover a large range of temperature on the domain of mass density considered. The EOSs of hydrogen and tritium above 1 eV and above, respectively, 0.1 g/cm^3 and 0.3 g/cm^3, can be obtained from the EOS of deuterium above 1 eV and 0.2 g/cm^3 by the scaling law described in Ref. [15].

In the thermodynamic domain considered, the assumptions underlying our approach (nonrelativistic electrons, classical nuclei, Born-Oppenheimer hypothesis) seem relevant so that the only approximation lies in the choice of the electron exchange-correlation functional F_{xc}. The GGA functional [51] is widely used to calculate the EOS of dense plasmas with QMD. In order to compare our EOS of deuterium, denoted QOFWH, with other works, we have implemented it with GGA corrected to approximately include the influence of temperature. The influence of T in F_{xc} turns out to be small, 2% at most for pressure in the thermodynamic domain considered.

The pressures obtained with QOFWH have been compared to those obtained with Kerley03, with PIMC, and with the fit of Caillabet *et al.* Kerley03 is a chemical model [53], PIMC is an *ab initio* approach that needs no approximation for F_{xc} but that cannot be applied below one-tenth of the Fermi temperature [1], and the fit of Caillabet *et al.* is constructed with QMD results obtained below 0.9 eV and with PIMC results obtained above 1 eV [15]. For the most part, Kerley03 [53] is in good agreement with QOFWH except at low temperature and low or intermediate mass density. The fit of Caillabet *et al.* differs by up to 11% from QOFWH. It also differs by up to 24% from PIMC; this result is surprising as the fit is constructed, above 1 eV, from PIMC data. The comparison of PIMC and QOFWH shows that the two *ab initio* approaches are in good agreement above 10 eV, which induces us to think that they both give reliable results in this domain; some significant differences occur, however, at low temperature and low or intermediate mass density.

Whether the discrepancies between the *ab initio* approaches QOFWH and PIMC stem from the choice of F_{xc} or from a numerical problem in PIMC remains to be known. It can be noted, however, that the discrepancies observed occur mainly in a domain where the sensitivity of QOFWH to exchange correlation, if it is measured by the difference between GGA and LDA for pressure, turns out to be small and where the statistical error on PIMC results is much larger than the statistical error on QOFWH results. Future work could therefore consist in revisiting PIMC at the conditions where large differences with QOFWH occur. It could also consist in applying our approach to an element with a higher atomic number and in comparing the results with other *ab initio* approaches, particularly with PIMC.

ACKNOWLEDGMENT

[1] S. X. Hu, B. Militzer, V. N. Goncharov, and S. Skupsky, Phys. Rev. B **84**, 224109 (2011).

[2] D. Saumon and G. Chabrier, Phys. Rev. A **46**, 2084 (1992).

[3] M. Ross, Phys. Rev. B **58**, 669 (1998).

[4] F. J. Rogers, Contrib. Plasma Phys. **41**, 179 (2001).

[5] H. Juranek, R. Redmer, and Y. Rosenfeld, J. Chem. Phys. **117**, 1768 (2002).

[6] M. A. Morales, C. Pierleoni, and D. M. Ceperley, Phys. Rev. E **81**, 021202 (2010).

[7] B. Militzer and D. M. Ceperley, Phys. Rev. Lett. **85**, 1890 (2000).

[8] B. Militzer and D. M. Ceperley, Phys. Rev. E **63**, 066404 (2001).

[9] B. Militzer, D. M. Ceperley, J. D. Kress, J. D. Johnson, L. A. Collins, and S. Mazevet, Phys. Rev. Lett. **87**, 275502 (2001).

[10] T. J. Lenosky, S. R. Bickham, J. D. Kress, and L. A. Collins, Phys. Rev. B **61**, 1 (2000).

[11] G. Galli, R. Q. Hood, A. U. Hazi, and F. Gygi, Phys. Rev. B **61**, 909 (2000).

[12] L. A. Collins, S. R. Bickham, J. D. Kress, S. Mazevet, T. J. Lenosky, N. J. Troullier, and W. Windl, Phys. Rev. B **63**, 184110 (2001).

[13] M. P. Desjarlais, Phys. Rev. B **68**, 064204 (2003).

[14] B. Holst, R. Redmer, and M. P. Desjarlais, Phys. Rev. B **77**, 184201 (2008).

[15] L. Caillabet, S. Mazevet, and P. Loubeyre, Phys. Rev. B **83**, 094101 (2011).

[16] J. M. Haile, *Molecular Dynamics Simulation* (Wiley-Interscience, New York, 1997).

[17] W. Kohn and L. J. Sham, Phys. Rev. **140**, A1133 (1965).

[18] N. D. Mermin, Phys. Rev. **137**, A1441 (1965).

[19] U. Gupta and A. K. Rajagopal, Phys. Rep. **87**, 259 (1982).

[20] R. G. Parr and W. Yang, *Density-Functional Theory of Atoms and Molecules* (Oxford University Press, New York, 1989).

[21] L. X. Benedict, K. P. Driver, S. Hamel, B. Militzer, T. Qi, A. A. Correa, A. Saul, and E. Schwegler, Phys. Rev. B **89**, 224109 (2014).

[22] K. P. Driver and B. Militzer, Phys. Rev. B **91**, 045103 (2015).

[23] F. Perrot, Phys. Rev. A **20**, 586 (1979).

[24] J.-F. Danel, L. Kazandjian, and G. Zérah, Phys. Plasmas **19**, 122712 (2012).

[25] T. Blenski and B. Cichocki, Phys. Rev. E **75**, 056402 (2007).

[26] T. Blenski and B. Cichocki, High Energy Density Phys. **3**, 34 (2007).

[27] R. Piron and T. Blenski, Phys. Rev. E **83**, 026403 (2011).

[28] D. A. Liberman, Phys. Rev. B **20**, 4981 (1979).

[29] J.-F. Danel, P. Blottiau, L. Kazandjian, R. Piron, and M. Torrent, Phys. Plasmas **21**, 102701 (2014).

[30] X. Gonze, J.-M. Beuken, R. Caracas, F. Detraux, M. Fuchs, G.-M. Rignanese, L. Sindic, M. Verstraete, G. Zérah, F. Jollet *et al.*, Comput. Mater. Sci. **25**, 478 (2002).

[31] X. Gonze, G.-M. Rignanese, M. Verstraete, J.-M. Beuken, Y. Pouillon, R. Caracas, F. Jollet, M. Torrent, G. Zérah, M. Mikami *et al.*, Z. Kristallogr. **220**, 558 (2005).

[32] X. Gonze, B. Amadon, P.-M. Anglade, J.-M. Beuken, F. Bottin, P. Boulanger, F. Bruneval, D. Caliste, R. Caracas, M. Côté *et al.*, Comput. Phys. Commun. **180**, 2582 (2009).

[33] F. Bottin, S. Leroux, A. Knyazev, and G. Zérah, Comput. Mater. Sci. **42**, 329 (2008).

[34] D. A. McQuarrie, *Statistical Mechanics* (University Science Books, Sausalito, CA, 2000).

[35] F. Zhang, J. Chem. Phys. **106**, 6102 (1997).

[36] P. Minary, G. J. Martyna, and M. E. Tuckerman, J. Chem. Phys. **118**, 2510 (2003).

[37] J.-F. Danel, L. Kazandjian, and G. Zérah, Phys. Rev. E **79**, 066408 (2009).

[38] F. Lambert, J. G. Clérouin, and G. Zérah, Phys. Rev. E **73**, 016403 (2006).

[39] J.-F. Danel, L. Kazandjian, and G. Zérah, Phys. Plasmas **15**, 072704 (2008).

[40] J.-F. Danel, L. Kazandjian, and G. Zérah, Phys. Plasmas **13**, 092701 (2006).

[41] O. H. Nielsen and R. M. Martin, Phys. Rev. B **32**, 3792 (1985).

[42] A. Dal Corso and R. Resta, Phys. Rev. B **50**, 4327 (1994).

[43] M. C. Payne, M. P. Teter, D. C. Allan, T. A. Arias, and J. D. Joannopoulos, Rev. Mod. Phys. **64**, 1045 (1992).

[44] P. E. Blöchl, Phys. Rev. B **50**, 17953 (1994).

[45] M. Torrent, F. Jollet, F. Bottin, G. Zérah, and X. Gonze, Comput. Mater. Sci. **42**, 337 (2008).

[46] N. A. W. Holzwarth, A. R. Tackett, and G. E. Matthews, Comput. Phys. Commun. **135**, 329 (2001).

[47] J. P. Perdew and Y. Wang, Phys. Rev. B **45**, 13244 (1992).

[48] J. C. Slater and H. M. Krutter, Phys. Rev. **47**, 559 (1935).

[49] R. P. Feynman, N. Metropolis, and E. Teller, Phys. Rev. **75**, 1561 (1949).

[50] B. U. Felderhof, G. W. Ford, and E. G. D. Cohen, J. Stat. Phys. **28**, 135 (1982).

[51] J. P. Perdew, K. Burke, and M. Ernzerhof, Phys. Rev. Lett. **77**, 3865 (1996).

[52] S. Ichimaru, H. Iyetomi, and S. Tanaka, Phys. Rep. **149**, 91 (1987).

[53] G. I. Kerley, Sandia National Laboratory Report No. SAND2003-3613 (2003).

[54] M. D. Knudson, D. L. Hanson, J. E. Bailey, C. A. Hall, J. R. Asay, and C. Deeney, Phys. Rev. B **69**, 144209 (2004).

[55] D. G. Hicks, T. R. Boehly, P. M. Celliers, J. H. Eggert, S. J. Moon, D. D. Meyerhofer, and G. W. Collins, Phys. Rev. B **79**, 014112 (2009).